Analysis of Torque Capacities in Hybrid Actuation for Human-Friendly Robot Design

Dongjun Shin[1], Fabian Seitz[1,2], Oussama Khatib[1], Mark Cutkosky[3]

[1]*Artificial Intelligence Laboratory, Stanford University, Stanford, CA 94305*
[2]*Autonomous Systems Lab, ETH Zurich, 8092 Zurich, Switzerland*
[3]*Mechanical Engineering, Stanford University, Stanford, CA 94305*
djshin@robotics.stanford.edu

Abstract— A formidable challenge in the development of human-friendly robots is to simultaneously achieve desired levels of performance and safety. To address this issue, a hybrid actuation concept has been proposed, combining large, low impedance actuators and small, high-frequency actuators. However, the determination of design parameters remains a challenge, as stiffness and electrical motor torque capacity simultaneously affect both the control performance and the safety of the manipulator. Using analytical models of the hybrid actuation system, we propose a methodology to achieve a combination of low impedance and high control bandwidth. The optimized parameters are verified and compared with previous ones through simulation and experimentation.

I. INTRODUCTION

A. Human-Friendly Robot

There is strong demand for emerging applications with human-friendly robots that can operate in close proximity with humans. However, most commercial robots are deployed in restricted environments where physical interaction between robots and humans is strictly regulated. The hardest challenge in developing human-friendly robots which support a variety of commercial uses is how to achieve the competing objectives of safety and performance. Previous efforts to address this trade-off between safety and control performance have included relocating the actuators to the base and powering the joints with cables (PaCMMA) [9] and employing a series elastic actuator (SEA) [11]. Zinn took advantage of both PaCMMA and SEA [18]. Other studies have employed variable stiffness [4] and links with high-strength composite materials to minimize inertia [2]. The robot safety is rigorously evaluated with crash tests [7].

The Stanford Safety Robot ($S2\rho$) (Fig. 1) has been designed to address the trade-off between performance and safety in robots intended for human interaction. Combining powerful pneumatic actuators with small electrical actuators in a parallel configuration at each joint, $S2\rho$ shows significant performance improvement over robots that solely use pneumatic actuation. At the same time, safety characteristics of $S2\rho$ are comparable to those of a human [13], [14].

B. Stiffness vs. Mini Actuator Torque Capacity

Low impedance output is essential for hybrid actuation to achieve safe manipulation. Many research efforts have
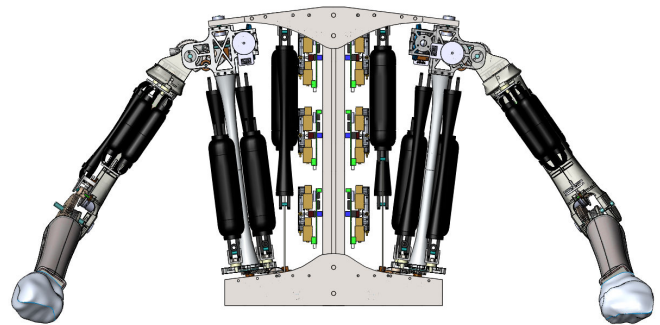

Fig. 1. The upper body portion of Stanford Safety Robot ($S2\rho$), which employs hybrid actuation (artificial pneumatic muscles and electromagnetic motor) with impact reducing sensor-embedded skin.

addressed minimizing impedance to obtain safe manipulation [8], [6], [18], [17]. Typically, the low impedance output is achieved by low stiffness, damping and inertia. While the low stiffness plays an important role to robot safety, this is in opposition to high control performance in terms of the position tracking bandwidth. Even high stiffness, using pneumatic muscles in a hybrid actuation scheme, does not guarantee high performance since high pressure increases nonlinear effects such as friction and hysteresis. Therefore, the relationship between joint stiffness by an antagonistic pair of muscles and control bandwidth needs to be investigated in a dynamic simulation in order to find the optimized stiffness for requirements of safety and performance.

Low reflected inertia is also important for low impedance output, particularly in high frequency impact. However, low reflected inertia achieved by a small actuator and lower gear ratio results in insufficient torque and acceleration, which mitigate the control performance as investigated in [12]. Furthermore, control bandwidth is affected by neither mere stiffness nor motor torque capacity alone, but both simultaneously. Optimal motor torque capacity for high control bandwidth is correlated to joint stiffness by an antagonistic pair of muscles. Therefore, it is necessary to investigate the relationship between stiffness and motor torque capacity. In this paper, we focus on the elbow joint for modeling, analysis, and evaluation. Section II presents the hybrid

actuation dynamic model, including pressure regulator and pneumatic muscles, in order to analyze and simulate the system. The optimization methodology is provided in Section III, followed by application and experimental evaluation in Section IV. Finally, the paper provides a conclusion and discussion of future work in Section V.

II. MODELING THE ROBOTIC MANIPULATOR

In order to determine the optimal motor torque capacity with a given joint stiffness by an antagonistic pair of muscles, it is essential to establish the general mathematical model of the robotic manipulator, under hybrid actuation.

A. System Modeling

The models are structured into the macro actuation by pneumatic muscles, the mini actuation by an electrical motor, and the combination represented as hybrid actuation.

The joint dynamics can be defined as:

$$\begin{cases} I_{eff}\ddot{q} + B\dot{q} + Mgd\cos(q) = \tau_M + \tau_m \\ I_{eff} = I_l + N^2 I_m \\ \tau_M = (F_1 - F_2)R \end{cases} \quad (1)$$

where I_l and I_m are the inertia of the link and motor, N is the gear ratio, B is a viscous damping coefficient, q is the joint angle, τ_M is the macro torque, τ_m is the mini torque, M is the mass of the link, F_i is the muscle force, d is the distance from the joint axis to the center of mass of the link, and R is the pulley radius.

1) Macro Actuation: The simplified static model of pneumatic muscle actuators was demonstrated by Hannaford and Chou [5] as follows:

$$\begin{cases} F_i = K_g(P_i - P_a)(L_i - L_m) + F_a \\ L_i = L_0 \mp Rq \end{cases} \quad (2)$$

where K_g, P_i, L_0, and L_i are stiffness per unit pressure, the internal gas pressure, the initial, and current muscle length, respectively. The remaining parameters are experimentally obtained as: $K_g = 0.0224m$, $P_a = -1.8250e4Pa$, $F_a = -22.1505N$, and $L_m = 0.1056m$.

For a typical proportional valve, the air flow through the orifice is controlled by adjusting the valve spool displacement. We assume the dynamics of the valve spool are fast enough to disregard. Hence, the air mass flow through the pneumatic valve is a function in terms of the input command and the ratio between inlet and outlet pressure. Based on ideal gas assumption, the air mass flow through the valve can be formulated as [3]:

$$\dot{m} = A(u)\Psi(P_u, P_d)C_d\sqrt{\frac{2}{R'T}}p_u \quad (3)$$

$$\Psi(P_u, P_d) = \begin{cases} \sqrt{\frac{\gamma}{\gamma-1}\left[\frac{p_d}{p_u}^{\frac{2}{\gamma}} - \frac{p_d}{p_u}^{\frac{\gamma+1}{\gamma}}\right]} & \text{for } \frac{p_d}{p_u} > 0.528 \\ \sqrt{\frac{\gamma}{\gamma+1}\left(\frac{2}{\gamma+1}\right)^{\frac{1}{\gamma-1}}} & \text{for } \frac{p_d}{p_u} \leq 0.528 \end{cases} \quad (4)$$

where A is the valve area dependent on the input command u, C_d is the discharge coefficient for the valve, and P_u and P_d are the upstream and downstream pressure, respectively. R' is the universal gas constant, T is the temperature at the valve orifice, and γ is the specific heat ratio. In order to increase the model accuracy, a different discharge coefficient is used for pressurizing and exhausting process. The coefficients are experimentally obtained as $C_{dpr} = 0.749$ and $C_{dex} = 0.676$.

Assuming muscle pressurizing and depressurizing undergoes an ideal and isothermal process, the pressure change in each muscle can be described as [15]:

$$\dot{P}_i = \frac{R'T}{V_i}\dot{m}_i - \frac{P_i}{V_i}\dot{V}_i \quad (5)$$

where P_i is the absolute pressure in each muscle, $\dot{m}_i$ is the flow rate and V_i is the volume which is dependent on the current contraction rate of each muscle. Due to the conclusion of [15], the volume shows a nearly linear behavior and can be assumed by the following expression:

$$\begin{cases} V_i(q) = A_v\epsilon_i(q) + V_0 \\ \epsilon_i(q) = \pm\frac{Rq}{L_0} \end{cases} \quad (6)$$

where ϵ_i is the muscle contraction. The constants were found as $A_v = 1.0348e-4m^3$ and $V_0 = 4.3530e-5m^3$.

2) Mini Actuation: Since the acceleration of the electrical motor is lower the faster the motor turns, the run-up time, Δt, at constant voltage up to the operating point is based on the mechanical time constant, τ_{MT}, no-load speed, n_0, operating speed, n_B, stall torque, M_H and operating torque, M_B of the motor [10].

$$\Delta t = \tau_{MT} \cdot \ln\frac{\left(1 - \frac{M_B}{M_H}\right)n_0}{\left(1 - \frac{M_B}{M_H}\right)n_0 - n_B} \quad (7)$$

3) Hybrid Actuation: The general hybrid actuation model consists of the linear combination of the torques (τ_M, τ_m) produced by the macro and mini actuation, respectively, as illustrated in Fig. 2. By closing the control loop around the pneumatic muscle through a load cell, the macro controller compensates for the pneumatic muscle force/displacement hysteresis phenomenon while also increasing the actuation bandwidth. The mini actuation with an open-loop torque controller compensates for the slow dynamics of the pneumatic muscle, allowing the hybrid actuation to achieve a higher frequency control bandwidth. In order to analyze the impedance and position control bandwidth for the macro, mini or hybrid actuation, a position tracking controller was implemented as an outer loop.

B. Mechanical Impedance

In order to establish an analytical way to describe how the stiffness by an antagonistic pair of muscles affects safety and performance, an appropriate LTI model and its associated transfer function have been taken into account. The antagonistic McKibben muscle actuator is a system with two inputs of the valve commands and one output of the joint
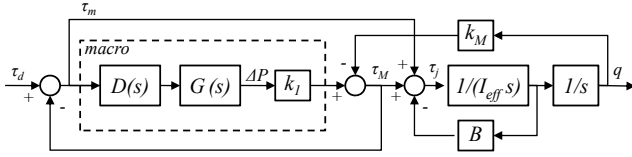
Fig. 2. LTI model of the Hybrid Actuation. The block $D(s)$ represents the macro controller while $G(s)$ describes the muscle dynamic.
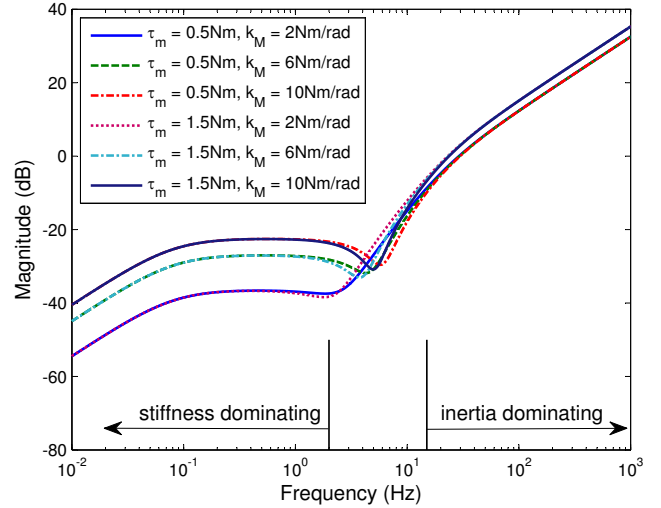

Fig. 3. Impedance with respect to stiffness and inertia. Stiffness dominates impedance at lower frequency, while inertia by motor size dominates impedance at higher frequency. Both stiffness and inertia adequately contribute at intermediate frequency.

angle. If the initial tension of each muscle is included in the model, a specific initial force must be added to the desired input signal for the closed-loop macro control which results in a nonlinear system.

However, the SISO model presented by Tondu and Lopez [16] uses the pressure difference ΔP between the two muscles as an input variable and includes the initial pressure (which is assumed to be proportional to the initial tension) in a separate restoring torque term:

$$\begin{cases} \tau_M = k_1 \Delta P - k_M q \\ k_1 = 2K_1, \ k_M = 2K_2 P_0 \\ K_1 = (\pi r_0^2)R[a(1 - k\epsilon_0)^2 - b] \\ K_2 = (\pi r_0^2)R2a(1 - k\epsilon_0)kR/l_0 \\ a = 3/\tan(\alpha_0)^2, \ b = 1/\sin(\alpha_0)^2 \end{cases} \quad (8)$$

where r_0, α_0, k, ϵ_0, k_1, and k_M are the initial muscle radius, the initial braid angle, the correction parameter ($k \leq 1.35$), the initial contraction, and the joint stiffness by an antagonistic pair of muscles, respectively. The parameters were experimentally obtained as: $r_0 = 0.0100m$, $\alpha_0 = 38.6142°$, $k = 1.1021$ and $\epsilon_0 = 0.1200$.

Based on equation 8, the closed-loop hybrid actuation model can be obtained by the LTI model as shown in Fig. 2. In this model the macro controller, $D(s)$, represents a simple PID controller which converts the torque error into a mass-flow proportional output. The function, $G(s)$, describes the first-order muscle dynamic which provides ΔP based on equation (5). Due to the limited possibilities in modeling linear systems, the mini torque τ_m includes no motor saturation model and is represented as the torque error which is directly applied at the joint.

Based on this linear closed-loop model, the following transfer function for the impedance can be developed:

$$Z(s)_{closed-loop} = \frac{\tau_M(s)}{\dot{q}(s)} = \frac{-I_{eff}s - B - k_M/s}{1 + k_1 D(s)G(s)} \quad (9)$$

where I_{eff}, B, and k_M are the effective inertia, the damping coefficient, and the joint stiffness by an antagonistic pair of muscles.

III. OPTIMIZATION FOR SAFETY AND PERFORMANCE

Robot safety and performance are competing objectives and depend upon the joint stiffness, k_M, and effective inertia, I_{eff}. However, the trade-off between these objectives is complicated. Since the effective inertia and stiffness simultaneously affect impedance output, low effective inertia

with small actuator torque capacity cannot guarantee the low impedance output, where the effective inertia has an empirical linear relationship with the mini actuator torque capacity [12]. Furthermore, although high stiffness typically provides high control bandwidth, high muscle pressure for high stiffness decreases control performance due to increased nonlinearity. To achieve both objectives of safety and performance, we first evaluate the mechanical impedance and the control bandwidth, and then find the optimal stiffness and mini actuator torque capacity.

A. Safety: Impedance vs. Stiffness vs. Mini Capacity

Mechanical impedance of the hybrid actuation is a function of effective inertia, damping, and stiffness as shown in equation (9). Fig. 3 shows that as the stiffness decreases at low frequency, so does the impedance. As the effective inertia increases at high frequency, which is the effect of increasing the mini actuator size, the impedance increases as well. In order to simplify the analysis, we sampled motor candidates and observed how the effective inertia varies with mini actuator torque capacity based on the empirical linear relationship [12]. Lower stiffness and inertia can provide safe manipulation with lower impedance, but the relationship among impedance, stiffness and inertia becomes more complicated at intermediate frequencies between 2Hz and 8Hz. Since closed-loop control bandwidth of the position tracking is placed around 6.4Hz, even well-designed collision avoidance algorithms cannot mitigate the danger of an unexpected crash. Therefore, we simulate and find the optimal combination of stiffness and inertia to minimize the impedance at each frequency based on equation (10) as shown in Fig. 4.
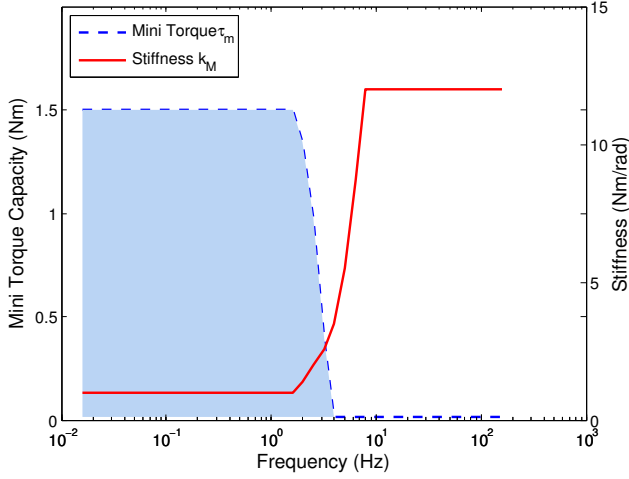
Fig. 4. A combination of stiffness and actuator torque capacity at each frequency in order to obtain minimum impedance. At low frequencies, the minimum impedance is obtained for the stiffness indicated and for all torques lesser than or equal to the torque indicated (shaded region). The result demonstrates that motor size does not significantly contribute to the minimum impedance output at low frequency.

$$\arg\min_{\tau_m, k_M} Z_{closed-loop} \qquad (10)$$

$$s.t. \qquad I_{eff} = I_L + N^2 I_m$$

$$I_m = 2.8e{-}4 \times \tau_m - 4.9e{-}6$$

$$0.015Nm \leq \tau_m \leq 1.5Nm$$

$$1Nm/rad \leq k_M \leq 12Nm/rad$$

where the boundaries of torque capacity, τ_M, and stiffness by an antagonistic pair of muscles, k_M, are determined by the muscle pressure range and suitable motor samples for the mini actuation, respectively.

The result shows that small mini actuator torque capacity is essential in order to obtain minimum impedance output at higher frequency than 6.4Hz, beyond which the hybrid actuation controller cannot effectively deal with an unexpected crash. However, since a lower impedance, achieved using smaller motor torque capacity, may also reduce the control performance, it is necessary to further investigate the relationship among control bandwidth, stiffness, and mini actuator torque capacity in order to seek optimal stiffness and mini actuator sizing for both safety and performance.

B. Performance: Bandwidth vs. Stiffness vs. Mini Capacity

A robotic manipulator driven by an antagonistic pair of pneumatic muscles has the ability to independently modulate its joint stiffness and joint torque. Since the maximum contraction of the pneumatic muscle is limited, and they should not be pressurized to more than 4 bar (58 psi) [1], the maximal feasible static stiffness can be calculated using equation (8) as $k_{Mmax} \cong 12Nm/rad$.

To obtain the optimal joint stiffness by macro actuation in terms of position control bandwidth, we conducted a simulation using Matlab/Simulink, where desired sinusoidal

position tracking with an amplitude of $\pm 5°$ and a joint stiffness range from 0 to k_{Mmax} has been carried out.

Furthermore, to determine an optimal mini actuator torque capacity on the basis of position control performance, different motor characteristics have been used in the hybrid actuation by increasing the maximum mini torque by an increment of 15mNm step by step.

Fig. 5 shows the results in the macro actuation and different motor torque capacities in the mini actuation. While the mini actuation is compensating the low dynamics of the pneumatic muscles, the performance of the hybrid actuation results in a noticeable higher bandwidth compared to the macro actuation. However, increasing stiffness beyond a certain value in the hybrid actuation causes considerable dropping in the position control bandwidth. Due to the time constant of joint and muscle dynamics, the hybrid actuation is associated with saturation in position control bandwidth at a certain frequency.

Note that the bandwidth at low stiffness, i.e., low operating pressure, is rather low since the pressure ratio of environmental pressure to muscle pressure is lower than the critical pressure ratio, $p_{crit} = (\frac{2}{n+1})^{\frac{n}{n-1}}$ [3], which causes a subsonic air mass flow out of the muscle. In order to avoid the same behavior at higher stiffness, the supply pressure, p_{supply}, should be higher or equal to $\frac{p_{max}}{p_{crit}}$ so that the air mass flow into the pneumatic muscle always remains a chocked flow.

In order to find a way to analytically describe the complexity of the interference between mini and macro actuation regarding the stiffness by an antagonistic pair of muscles, it is advantageous to develop a closed-loop position control transfer function for macro and mini actuation. By considering only macro actuation according to the LTI model (Fig. 2)
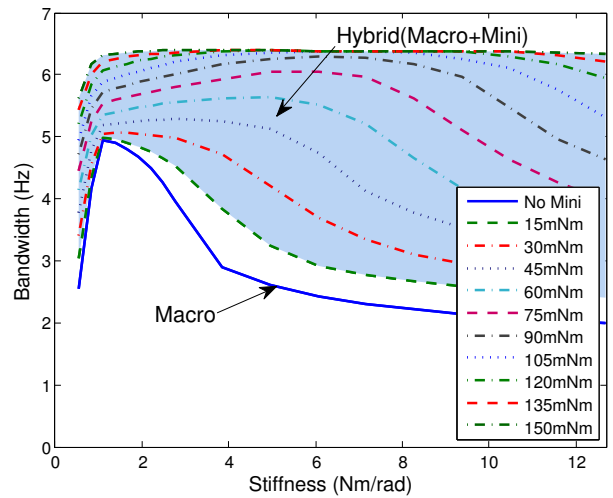

Fig. 5. Stiffness vs. position control bandwidth in macro alone and hybrid actuation. Simulation is performed over the entire range of feasible stiffness by an antagonistic pair of muscles, while varying the mini torque capacity. Beyond the torque capacity of $150mNm$, the hybrid actuation is associated with saturation in position control bandwidth at a certain frequency due to the time constant of joint and muscle dynamics.
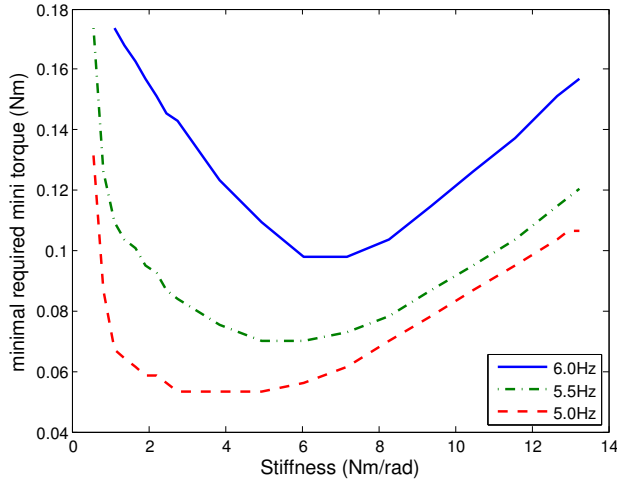
Fig. 6. Stiffness vs. minimal required mini torque capacity with respect to the different desired position control bandwidths: The minimal required torque capacity is strongly dependent on the stiffness by an antagonistic pair of muscles.
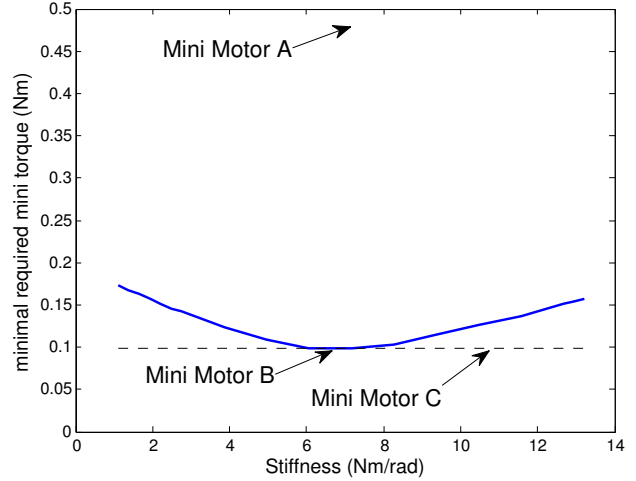

Fig. 7. Stiffness vs. minimal required mini torque capacity for position control bandwidth of 6Hz. Motor A and Motor B indicates the motor selection of current and optimized design, respectively. The optimized design improves safety characteristics by minimized inertia/weight of motor, yet maintains the same performance.

	Current Design (A)	Optimized Design (B)
Motor	RE26	RE25
Gearhead	14:1 (Two stages)	3.8:1 (One Stage)
Torque Capacity	482 mNm	98.8 mNm
Actuator Inertia	4.0360e-5 kgm^2	1.86640e-6 kgm^2
Actuator Weight	0.236 kg	0.105 kg

TABLE I. MINI ACTUATOR OPTIMIZATION AT A GIVEN STIFFNESS OF 6.5NM/RAD AND DESIRED POSITION CONTROL BANDWIDTH OF 6HZ.

described in the previous section and closing the outer loop by a PID controller $E(s)$, the following transfer function can be derived:

$$T_M(s) = \frac{E(s)S(s)}{A(s) + B(s) + C_M(s)} \qquad (11)$$

where $S(s) = D(s)G(s)k_1$, $A(s) = I_{eff}(1 + S(s))s^2$, $B(s) = B(1 + S(s))s$, and $C_M(s) = (E(s)S(s) + k_M)$.

For the hybrid actuation, the transfer function results in the following expression:

$$T_H(s) = \frac{(1 + S(s))E(s)}{A(s) + B(s) + C_H(s)} \qquad (12)$$

where $C_H(s) = (1 + S(s))E(s)$.

It is important to note, however, that the expressions above are based on a linear system and do not take into account that torque capacity is limited. By analyzing these two transfer functions, it can be shown that hybrid actuation is canceling stiffness terms in the denominator, which explains the saturation in position control bandwidth at a certain frequency over the whole range of stiffness, k_M. It should be noted that the maximum achievable bandwidth of 6.4Hz in the hybrid actuation can also be derived by using equation (12). The performance of the hybrid actuation increases up to the bandwidth saturation level, from which the open loop control of mini actuation suffers. Therefore, the minimal required mini torque to achieve a desired performance should be considered. Fig. 6 clearly shows that the required mini torque strongly depends on stiffness by an antagonistic pair of muscles.

IV. APPLICATIONS AND EXPERIMENTAL VERIFICATION

While a sophisticated controller such as collision avoidance algorithm can improve the safety below the closed-loop

control bandwidth, a controller cannot diminish the danger in unexpected crashes at higher frequency, at which higher inertia typically dominates impedance. Therefore, optimizing the effective inertia by a smaller actuator size has higher priority to decreasing the stiffness by an antagonistic pair of muscles. Choosing the optimal stiffness and mini actuator torque capacity (Motor B) shown in Fig. 7 guarantees maximum robot safety and a desired control bandwidth of 6Hz.

A. Comparison between Current and Optimized Design

Table I shows comparison of current actuator sizing and optimized one (Motor A and B, respectively in Fig. 7). While both actuators achieve the same desired position control bandwidth of 6Hz [14], the optimized design improves safety characteristics by minimized motor torque capacity and inertia/weight.

B. Experimental Verification

To validate the optimized design/control parameters of the hybrid actuation, experiments of position tracking at two different stiffnesses, by an antagonistic pair of muscles, were conducted at a elbow joint testbed (Fig. 8). As shown in Fig. 9, the hybrid actuation system achieves a desired bandwidth of 6Hz with optimized parameters of a stiffness of 6.5Nm/rad and a mini actuator torque of 0.1Nm (Motor B), while a
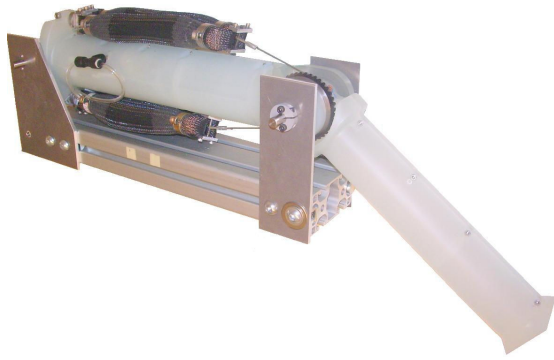
Fig. 8. Elbow Joint Testbed: an antagonistic pair of pneumatic muscles (macro actuation) and an electrical motor (mini actuation), which is enclosed in the link, are attached to the joint in parallel.

stiffness of 11Nm/rad with the same mini torque decreases the performance as simulated in Fig. 7 (Motor C).

V. CONCLUSION AND FUTURE WORK

In this paper, we developed an analytic model of the hybrid actuation system for human-friendly robot design and control. In order to find an effective solution for the complex trade-off between safety and performance, we investigated how the stiffness of an antagonistic pair of muscles and the mini actuator torque capacity contribute to overall mechanical impedance and control bandwidth. Based on this analysis, we proposed a methodology to optimize design parameters. The methodology provides optimal stiffness and mini actuator torque capacity, which achieves a desired control bandwidth with minimal impedance output. Chosen optimal parameters such as stiffness and mini actuator torque capacity show significant improvement to the previous design. All of these results were verified with experimental setup of an elbow joint in Stanford Safety Robot. These results are being used in 7 DOF Stanford Safety Robot, while taking into account motor saturation and a payload sensitivity analysis.

VI. ACKNOWLEDGMENTS

REFERENCES

[1] Website of shadow robot company ltd., united kingdom, http://www.shadowrobot.com.
[2] A. Albu-Schaffer and G. Hirzinger. State feedback controller for flexible joint robots: A globally stable approach implemented on dlr's lightweight robots. *Proc. of the 2000 IEEE/RSJ International Conf. on Intelligent Robots and Systems*, 2:1087–1094, 2000.
[3] P. Beater. Pneumatic drives. pages 25–39, 2007.
[4] A. Bicchi and G Tonietti. Fast and soft arm tactics: Dealing with the safety-performance trade-off in robot arms design and control. *IEEE Robotics and Automation Magazine*, 11:22–33, 2004.
[5] C. P. Chou and B. Hannaford. Measurement and modeling of mckibben pneumatic artificial muscles. *IEEE Robotics and Automation Magazine*, 12(1):90–102, 1996.
[6] J.P. Desai and R.D Howe. Towards the development of a humanoid arm by minimizing interaction forces through minimum impedance control. *IEEE Int. Conf. on Robotics and Automation*, 4:4214–4219, 2001.
[7] S. Haddadin, A. Albu Schaffer, and G. Hirzinger. Safety evaluation of physical human-robot interaction via crash testing. *Robotics: Science and Systems Conference*, 2007.
[8] N. Hogan. Impedance control: an approach to manipulation. *Journal of Dynamic Systems, Measurements and Control*, pages 1–24, 1985.
[9] J. B. Morrel. Parallel coupled micro-macro actuators. *PhD thesis, Massachusetts Institute of Technology, Cambridge, MA*, 1996.
[10] Maxon Motor. Program 05/06 of the leading supplier of high precision drives and systems. page 37, 2006.
[11] G. Pratt and M. Williamson. Series elastic actuators. *Proc. of the 1995 IEEE/RSJ International Conference on Intelligent Robots and Systems*, 1:399–406, 1995.
[12] D. Shin, M. Cutkosky, and O. Khatib. Design methodologies of a hybrid actuation approach for a human-friendly robot. *Proc. of the 2009 IEEE International Conference on Robotics and Automation*, 2009.
[13] D. Shin, I. Sardellitti, and O. Khatib. A hybrid actuation approach for human-friendly robot design. *Proc. of the 2008 IEEE International Conference on Robotics and Automation*, 2008.
[14] D. Shin, I. Sardellitti, Y. Park, O. Khatib, and M. Cutkosky. Design and control of a bio-inspired human-friendly robot. *The International Journal of Robotics Research OnlineFirst at http://ijr.sagepub.com/cgi/content/abstract/0278364909353956v1*, 2009.
[15] J.M. Zollner R. Dillmann T. Kerscher, J. Albiez. Evaluation of the dynamic model of fluidic muscles using quick-release. *The First IEEE/RAS-EMBS International Conference on Biomedical Robotics and Biomechatronics*, pages 637–642, 2006.
[16] B. Tondu and P. Lopez. Modeling and control of mckibben artificial muscle robot actuators. *IEEE Control Systems Magazine*, 30:15–38, 2000.
[17] Giovanni Tonietti, Riccardo Schiavi, and Antonio Bicchi. Optimal mechanical/control design for safe and fast robotics. *The 9th International Symposium on Experimental Robotics*, 21:311–320, 2004.
[18] M. Zinn, B. Roth, O. Khatib, and J. K. Salisbury. New actuation approach for human-friendly robot design. *International Journal of Robotics Research*, 23(1):379–398, 2004.
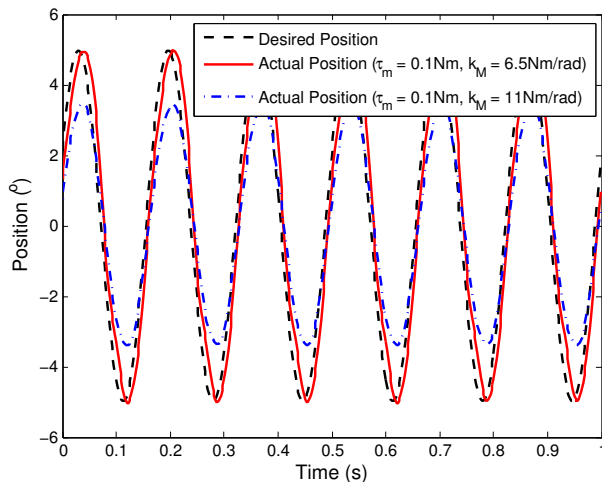
Fig. 9. Position Tracking Performance. The hybrid actuation system achieves the desired bandwidth of 6Hz with optimized parameters of stiffness of 6.5Nm/rad and mini actuator torque of 0.1Nm, while a stiffness of 11Nm/rad with the same mini torque decreases the performance.